# A new approach to contact angle measurement and effects of evaporation on the contact angle

M. Faruk Çakır

*Department of Electronic Automation, Vocational School, Çankırı Karatekin University, Çankırı, Turkey, Postal 2100.*

Received 25 December 2022; accepted 7 February 2024

The solid material's wettability behavior is determined by the contact angle value. The wettability of materials is critical in the coating, lubricating, and insulating industries. In high-tech industries including corrosion resistance, water-oil separation, medical material production, implant technology, and friction reduction, the contact angle is very important. A new method called the full angle method was used to measure the contact angle and compared with current methods. The wettability behavior of plexiglass, which is employed in a variety of applications ranging from lighting to decorating, and industrial designs to accessory production, was explored in this study. The measurement of the contact angle was done by dropping 1.8 M (molar) of saltwater over the plexiglass materials. In order to examine the effect of evaporation on the contact angle, changes in contact angle, height and baseline were investigated depending on the waiting time.

*Keywords:* Contact angle measuring system; full angle method; wettability; evaporation effect; contact angle.

DOI: https://doi.org/10.31349/RevMexFis.70.031002

## 1. Introduction

Measurement has emerged with the existence of human beings. At every stage of life, the concept of measurement continues to develop and maintain its importance. The wettability behavior of the materials is determined by making measurements. The absorption or pushing of liquid on solid materials is related to the wettability behavior. Hydrophobic and hydrophilic behavior occurs according to the value of the angle formed by the liquid, solid and air environments on the material, which is called the contact angle. In hydrophilic materials, the liquid wets the surface it contacts well, while in hydrophobic materials, the liquid is pushed by the surface it contacts. Surfaces with a contact angle of fewer than 90 degrees are considered hydrophilic and surface greater than 90 degrees are considered hydrophobic. Wettability behavior is of great importance in the design and production of any product with solid materials. The contact angle, which occurs when solids are wetted by liquids, has an important place in many application areas such as lubrication, coating, printing, waterproofing and detergent [1,2]. A wide range of applications has emerged, from materials such as self-cleaning glass by controlling wettability to high-tech areas such as microfluidic control, corrosion resistance, water-oil separation, medical material production, implant dental technology [3-7]. Researchers are working on increasing the wettability in order to ensure that the denture material can be better adhered to in the mouth. However, optical technology is one of the areas where wettability is widely used [8,9]. In addition, applications are made in various engineering fields such as biomaterials, construction materials, anti-corrosion coatings and implant technology [10-13]. The contact angle is the most important concept in determining the wettability behavior [14,15]. When the liquid is dripped onto the material, the liquid molecules pulled each other in the droplet. Liquid molecules on the solid surface are pulled only by solid molecules. This is because the potential energies of the surface molecules are lower than those of the molecules in the droplet. As a result, the molecules on the surface of the liquid form a denser layer. In this situation, the droplet takes the shape of a sphere with the contribution of gravity and open air pressure. Surface analysis researchers have done various technical and system development studies regarding standard contact angle and wettability [16-18]. Many techniques have been developed over the years. However, among these, Wilhelmy balance tensiometry (WBT) and contact angle goniometry have become standard methods and have gained a great reputation. Goniometers are systems that record and automatically analyze drop images in contact angle measurement experiments. Measurement with a goniometer is one of the most widely used contact angle measurement techniques. It measures the tangential angle formed at the three-phase contact point of a fixed drop [19]. The first commercial contact angle goniometer was designed and made by W.A. Zisman. Today, with the development of image processing and computer technology, goniometers have become very advanced and have become more sensitive and able to make measurements with very low error rates. In this study, a system was developed for contact angle measurement. Contact angle measurements were made with the system consisting of hardware and software. A new method called the full angle method was used for contact angle measurement. The wettability of the plexiglass material, which is widely used in the industry, with salt water was investigated. Approximately 20 microliters of 1.8 molar saline were dropped onto the plexiglass material. Measurements were made every minute after drop. Measurements were made 5 times and averaged. The contact angle, height, and baseline of the drop were measured. Information

about the wettability behavior of the plexiglass material with salt water was obtained.

## 2. Wettability behavior and contact angle

In 1805 Young found the relationship between the contact angle and the surface free energy of the solid. Young's studies form the basis of the studies on the wettability behavior of materials [20]. The contact angle is the angle formed by the materials in the solid, liquid and gas phases together with the effect of gravity. The magnitude of this angle depends on the size of the attraction forces between the molecules of the liquid (cohesion forces) and the attraction forces between the liquid and solid (adhesion forces). In addition, the gravitational force of the environment and the open-air pressure are the parameters affecting the contact angle. Fig. 1 shows the forces acting on the droplet and the contact angle.

In the calculation of contact angles, methods such as tangential method, Young-Laplace method, half-angle, ellipse and polynomial methods are used. In this study, a new contact angle measurement method called the full angle method (FAM) was used. In addition, measurements were made with the half-angle method in order to make comparisons. In the half-angle method, when the height $h$ formed by the drop on the solid surface and the base radius of the drop $r$ is taken the contact angle can be calculated as shown in Eq. (1) [21]. A schematic representation of the measurement of the contact angle with the half-angle method is given in Fig. 2.

$$\theta = 2\tan^{-1}\left(\frac{h}{r}\right), \tag{1}$$

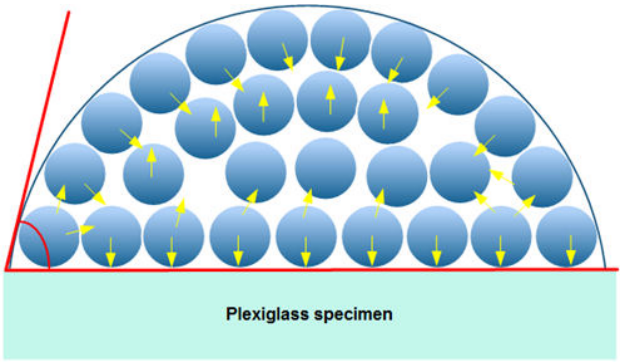


FIGURE 1. Schematic representation of the formation of spherical droplets with surface tensions.

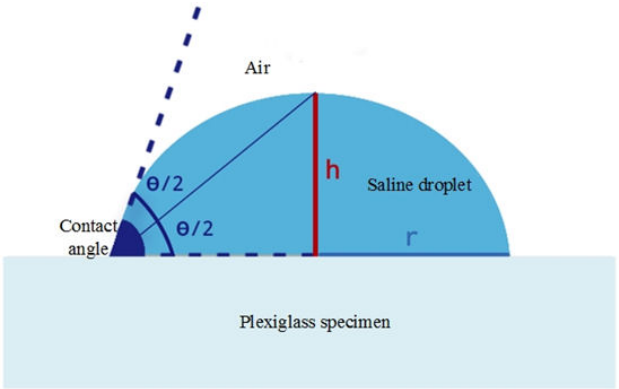


FIGURE 2. Schematic representation with the $\theta/2$ method for contact angle measurement.

### 2.1. New method (full angle method (FAM))

The schematic representation of the method we call the Full Angle Method (FAM) is given in Fig. 3.

Using the points.

Line equation passing through the points $A(x_1, y_1)$, $B(x_2, y_2)$ and $C(x_3, y_3)$.

length of line segment AB;

$$|AB| = \sqrt{(x_2 - x_1)^2 + (y_2 - y_1)^2}, \tag{2}$$

Line equation passing through the points $B(x_2, y_2)$ and $C(x_3, y_3)$

$$\frac{(y_3 - y_2)}{(x_3 - x_2)} = \frac{(y - y_3)}{(x - x_3)}, \tag{3}$$

using the expression

$$a.x + b.y + c = 0, \tag{4}$$

obtained. Using the expression of the distance of a point $A(x_1, y_1)$ to a line;

$$h = |AK| = \frac{|a.x_1 + b.y_1 + c|}{\sqrt{(a^2 + b^2)}}, \tag{5}$$

obtained. After calculating the length AB and AK,

$$\theta = \sin^{-1}\left(\frac{|AK|}{|AB|}\right), \tag{6}$$

angle value is found. The calculated angle indicates the contact angle value. When the contact angle value is greater than 90°, the Θ° value found by the FAM method is subtracted from 180° to obtain the contact angle value. Contact angle measurements were made with the computer program prepared using Eqs. (2-6). The realized contact angle measure-

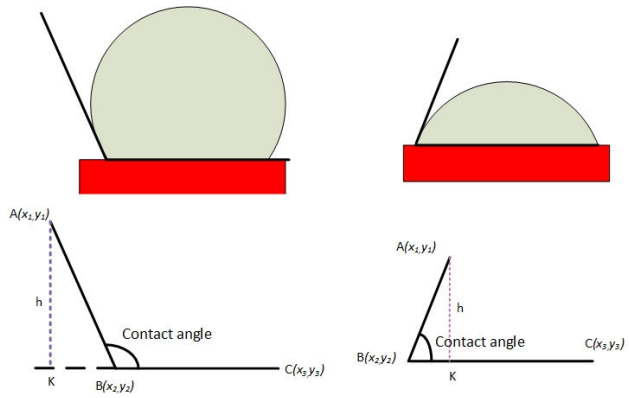


FIGURE 3. Schematic representation of the FAM.

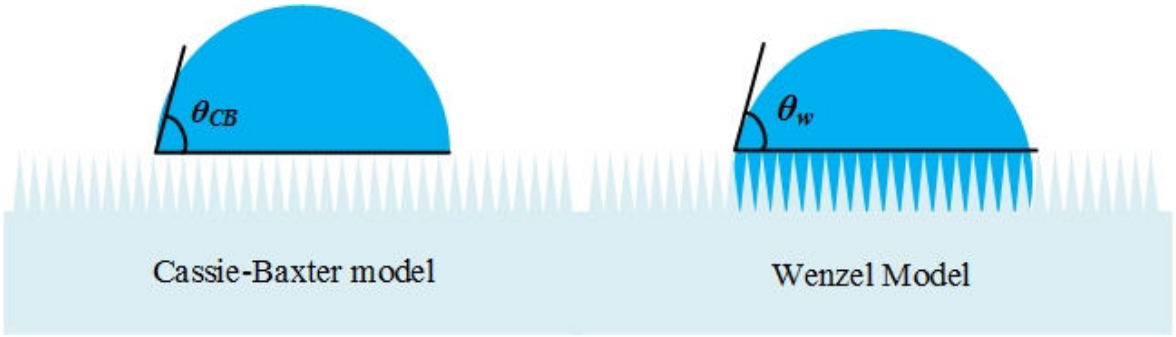


FIGURE 4. Schematic representation of Cassie-Baxter and Wenzel models.

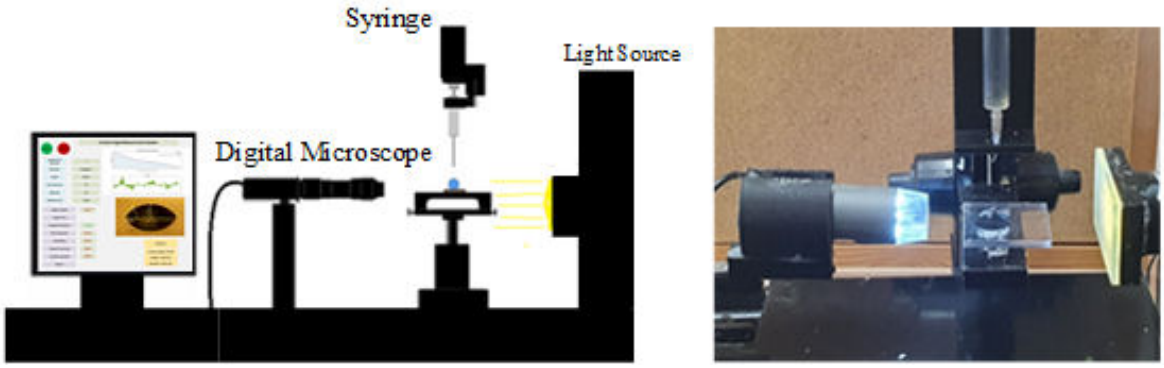


FIGURE 5. Schematic of contact angle measurement system.

ment system and program is very easy and practical. The most important point to be considered while measuring is to obtain the image of the drop on the surface and to determine the measurement points precisely. Determining the droplet's contact point with the solid surface is the most critical point of the measurement. The development of image acquisition technologies increases the quality of the images obtained.

### 2.2. Wettability behavior

Young's equation is used to study the wetting behavior of smooth solid surfaces. Two different wetting models are preferred, Wenzel (homogeneous wetting) and Cassie-Baxter (heterogeneous wetting) for wetting a rough surface [22]. The liquid is assumed to completely wet the rough solid surface in the Wenzel model. The roughness increases the wetting property of the solid surface. The Cassie-Baxter model is preferred with inhomogeneous rough solid surfaces. It is assumed that the air is trapped by the liquid in the valleys between the surface roughness in this model. A schematic representation of Cassie - Baxter and Wenzel models is given in Fig. 4. Cassie - Baxter model gives much more suitable results for real systems than Wenzel model.

## 3. Contact angle measurement system

A measuring system was made for contact angle measurements. It has been made at very affordable prices compared to the measurement systems sold in the market. The measurement system consists of software and hardware [23]. The mechanical parts of the hardware were made using a 3D printer The schematic of the contact angle measurement system is given in Fig. 5.

The use of the system and image analysis are performed in the software section. A clear image of the droplet is taken with the using of a digital microscope. Thanks to the prepared software, contact angle values are calculated and the desired reports are obtained. The user interface of the contact angle measurement system is shown in Fig. 6.

## 4. Experimental results

A measuring system was made for contact angle measurements. It has been made at very affordable prices compared to the measurement systems sold in the market. The measurement system consists of software and hardware [23]. The mechanical parts of the hardware were made using a 3D printer The schematic of the contact angle measurement system is given in Fig. 5. Images can be taken from the drop left on the solid surface at choosing time period with the help of the prepared interface. First of all, the identity information about the experiment is entered into the interface. One of the FAM or HAM methods should be selected for the measurement. When the droplet image is displayed on the screen, necessary actions must be taken for measurement by using the point selection, calculation and image processing buttons. The out-

TABLE I. Measured and averaged contact angle (FAM), Contact angle (HAM), baseline and height values.

| Wait (min) | Contact angle (FAM) | Contact angle (HAM) | Baseline (mm) | Height (mm) |
|---|---|---|---|---|
| 1 | 61.658 | 61.308 | 4.959 | 1.429 |
| 2 | 59.964 | 59.624 | 4.976 | 1.412 |
| 3 | 57.149 | 57.158 | 4.976 | 1.429 |
| 4 | 57.689 | 57.425 | 4.959 | 1.377 |
| 5 | 57.470 | 57.236 | 4.941 | 1.384 |
| 6 | 57.046 | 57.356 | 4.941 | 1.359 |
| 7 | 57.347 | 57.448 | 4.941 | 1.323 |
| 8 | 55.946 | 55.678 | 4.956 | 1.294 |
| 9 | 50.853 | 51.124 | 4.955 | 1.283 |
| 10 | 51.494 | 51.568 | 4.956 | 1.264 |
| 11 | 48.337 | 48.115 | 4.941 | 1.249 |
| 12 | 48.232 | 48.246 | 4.941 | 1.210 |
| 13 | 47.403 | 47.367 | 4.953 | 1.197 |
| 14 | 46.408 | 46.589 | 4.941 | 1.165 |
| 15 | 44.446 | 44.348 | 4.953 | 1.153 |
| 16 | 44.027 | 43.988 | 4.929 | 1.146 |
| 17 | 43.140 | 43.134 | 4.925 | 1.127 |
| 18 | 43.191 | 43.240 | 4.929 | 1.129 |
| 19 | 43.365 | 43.459 | 4.945 | 1.135 |
| 20 | 43.147 | 43.042 | 4.931 | 1.109 |
| 21 | 42.961 | 43.118 | 4.928 | 1.088 |
| 22 | 41.404 | 41.218 | 4.916 | 1.063 |
| 23 | 41.181 | 40.985 | 4.904 | 1.082 |
| 24 | 39.907 | 39.766 | 4.900 | 1.039 |
| 25 | 40.201 | 40.357 | 4.895 | 1.037 |
| 26 | 39.067 | 39.324 | 4.894 | 1.017 |
| 27 | 38.828 | 38.824 | 4.872 | 1.010 |
| 28 | 38.369 | 38.198 | 4.864 | 0.983 |
| 29 | 38.865 | 38.988 | 4.842 | 0.982 |
| 30 | 38.210 | 38.204 | 4.814 | 0.986 |
| 31 | 38.684 | 38.534 | 4.797 | 0.976 |
| 32 | 38.960 | 38.997 | 4.777 | 0.964 |
| 33 | 37.606 | 37.659 | 4.785 | 0.948 |
| 34 | 37.924 | 37.912 | 4.779 | 0.938 |
| 35 | 37.418 | 37.417 | 4.746 | 0.930 |
| 36 | 36.567 | 36.435 | 4.750 | 0.904 |
| 37 | 35.513 | 35.712 | 4.767 | 0.896 |
| 38 | 34.756 | 34.869 | 4.746 | 0.878 |
| 39 | 33.973 | 33.845 | 4.750 | 0.854 |
| 40 | 34.055 | 33.945 | 4.732 | 0.831 |
| 41 | 32.800 | 32.989 | 4.730 | 0.839 |
| 42 | 33.080 | 33.089 | 4.710 | 0.833 |
| 43 | 31.850 | 31.855 | 4.694 | 0.803 |
| 44 | 32.262 | 32.679 | 4.694 | 0.795 |
| 45 | 32.065 | 32.785 | 4.686 | 0.793 |
| 46 | 29.402 | 29.547 | 4.654 | 0.747 |
| 47 | 29.510 | 29.134 | 4.661 | 0.750 |
| 48 | 28.097 | 28.334 | 4.662 | 0.743 |
| 49 | 28.209 | 28.113 | 4.641 | 0.734 |
| 50 | 27.724 | 27.655 | 4.623 | 0.739 |
| 51 | 27.597 | 27.689 | 4.700 | 0.709 |
| 52 | 26.612 | 26.554 | 4.617 | 0.691 |
| 53 | 26.758 | 26.754 | 4.576 | 0.661 |
| 54 | 26.059 | 26.118 | 4.556 | 0.644 |
| 55 | 25.507 | 25.459 | 4.547 | 0.594 |
| 56 | 25.100 | 25.256 | 4.536 | 0.581 |

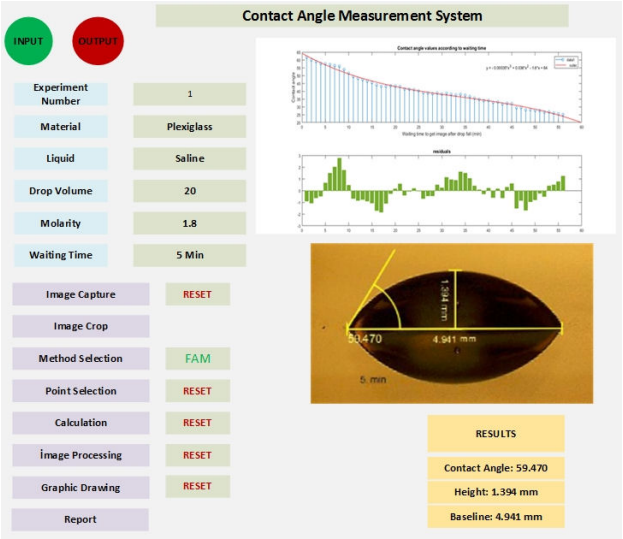


FIGURE 6. User interface view of contact angle measurement system.

put of the results in the form of reports and graphically is also provided by the use of the interface. The operations performed can be stored in the memory and other comparisons can be made with the next measurements. Approximately 20 microliters of 1.8 M saline were dropped onto the Plexiglas sample. After 1.8 M saline was dropped onto the plexiglass sample, droplet images were taken at one-minute intervals. The contact angle value was calculated with two different methods, the full angle method and the half-angle method. In addition, the height and baseline of each droplet were calculated. This measurement process was repeated 5 times for each drop. Table I was obtained by averaging the contact angle, drop height and baseline.

Contact angle measurements were made separately with the full-angle method and the half-angle method. When 5 different measurements are made for the 5th minute with the full angle method and averaged, the contact angle value is CA(5 min.)= 59.470°, the drop height $h$(5 min.)=1,394 mm, and the base length mm $l$(5 dk.)= 4,941 mm obtained. Similarly, the average values obtained for the waiting times of the 5th, 10th, 20th, 30th, 40th, 50th and 56th minutes are shown

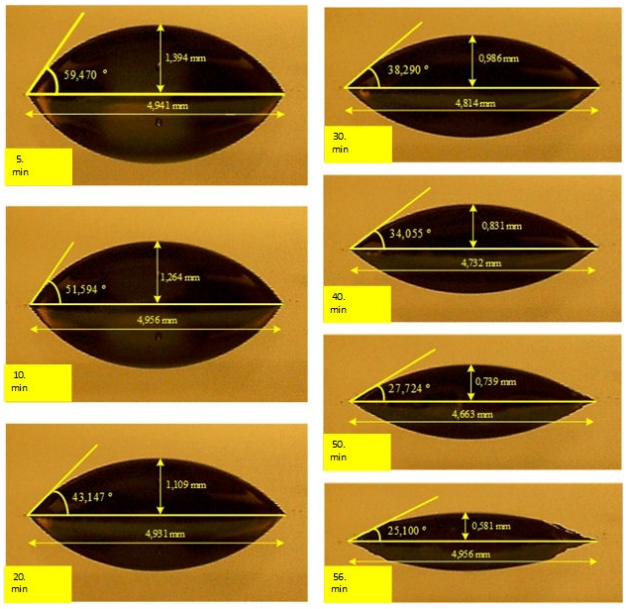


FIGURE 7. Droplet contact angle, height, and baseline values at specific times.

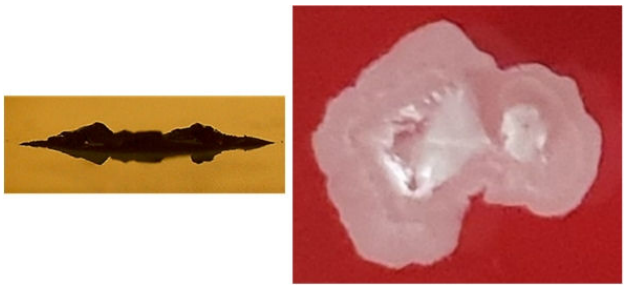

FIGURE 8. Side and top view of the droplet at the 67th minute.

in Fig. 7. After the 56th minute, the droplet started to deteriorate and the contact angle, drop height and base length could not be calculated. At the 67th minute, the water in the droplet evaporated completely and the form shown in Fig. 8 was displayed.

The saltwater dropped on the Plexiglass material evaporates after about 67 minutes, leaving only salt stacks and rings on the surface. When the water molecules in the droplet evaporate, the form of the salt crystals remaining on the plexiglass sample is not similar. Each droplet has a different character. The salt stacks seem to have inclined to drift towards the center. The relationship between contact angle and waiting time, according to the values obtained by the FAM method, is shown in Fig. 9. When the graph in Fig. 9 is examined, it is seen that the contact angle did not change rapidly until the 8th minute, but the error value was high. In addition, it is seen that the measurements around the 25th minute and 40th minute are more linear. The maximum error values between the function obtained from the third order and the measurement values are less than 3%. In other words, the change in the contact angle according to the waiting time has a very functional structure. In other words, the change in the contact angle according to the waiting time has a very functional structure. The equation of the relationship between contact angle and waiting time is given in Eq. (7).

$$f_{C.A} = -0.00035 * t^3 + 0.0036 * t^2 - 1.6 * t + 64. \quad (7)$$

The graph of the change between the baseline and the waiting time on the plexiglass material that the droplet contacts is given in Fig. 10. It is seen that there is very little change until the 25th minute. The error values between the obtained baseline and waiting time function and the measurement values are less than $\pm 0.1$. The very small values of the

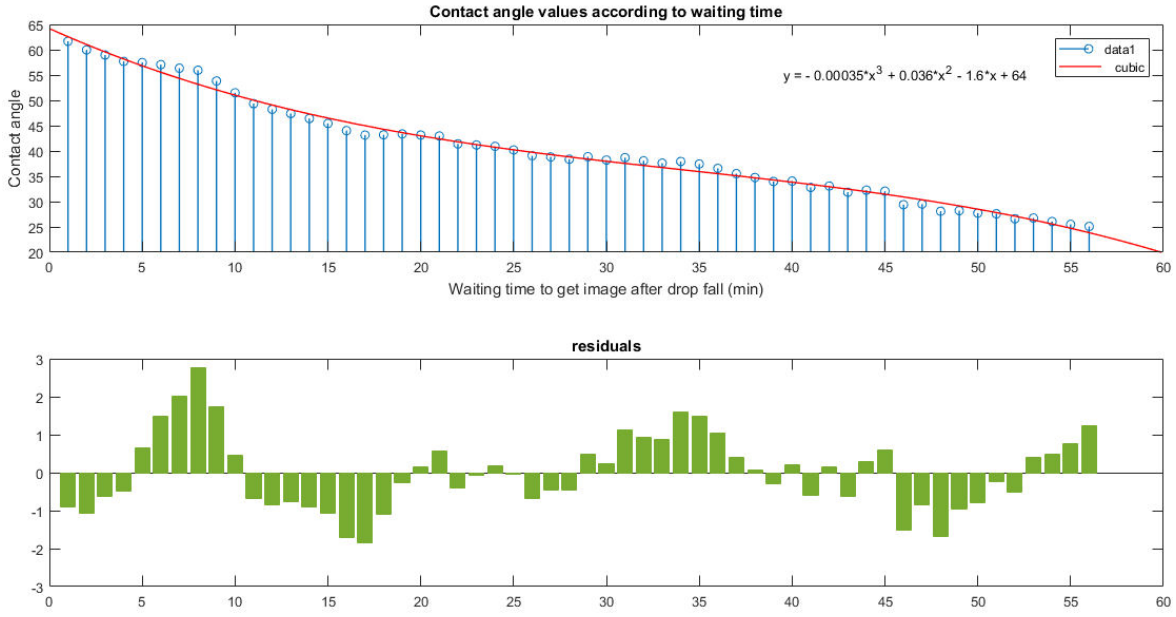


FIGURE 9. Change of contact angle according to waiting time.

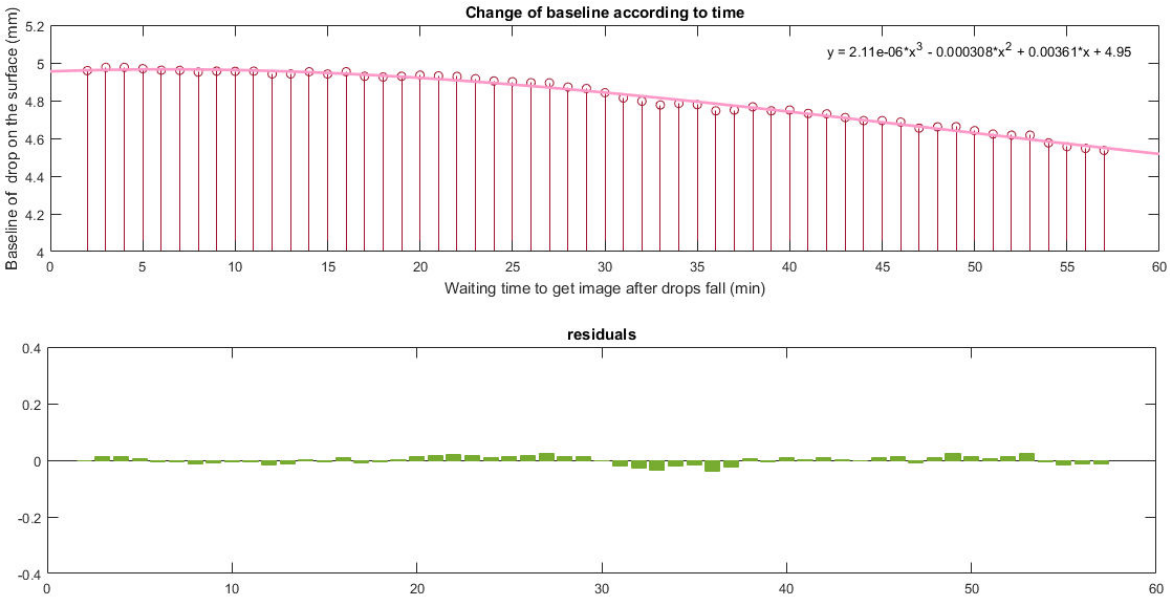


FIGURE 10. Change of baseline with waiting time.

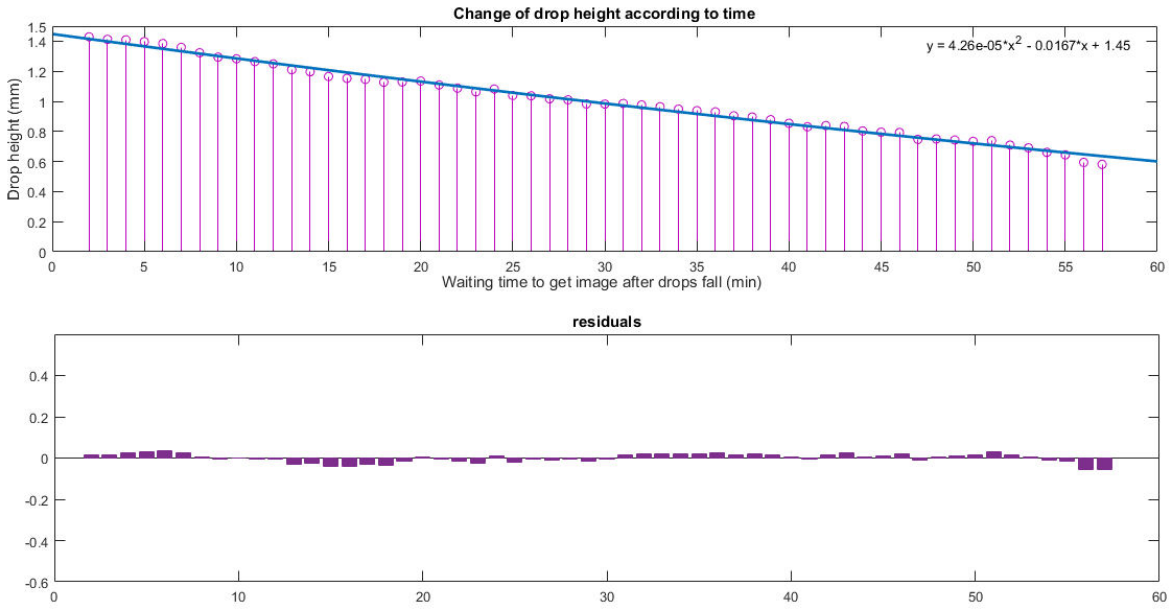


FIGURE 11. Change of droplet height with waiting time.

residuals indicate the suitability of showing made measurements with mathematical equations. The change of the droplet baseline with time is given in Eq. (8).

$$f_{BL} = 2.11 * 10^{-6} * t^3 - 0.000308 * t^2 + 0.00361 * t + 4.95. \quad (8)$$

The change in the height of the droplet above the plexiglass material with the waiting time is shown in Fig. 11. It is seen that the residuals values between the measurement values and the mathematical function obtained are quite small. The function is understood to be close to linear. The change of droplet height with waiting time is shown in Eq. (9).

$$f_h = 4.26 * 10^{-5} * t^2 - 0.00167 * t + 1.45. \quad (9)$$

## 5. Conclusions

A new measurement method called the full angle method (FAM) has been developed for contact angle measurements. In addition, a very cost-effective measurement system was made to make the measurements. The most important point to be considered in the FAM method is to determine the con-

tact point of the droplet. After the tangent point is determined without error, the contact angle is calculated with the three points determined independently from the measurement height and base radius values. For the accuracy control of the FAM measurement method, contact angle measurements of the same droplets were made with the half-angle method. It has been observed that the measurement results of the two measurement methods are very close to each other. After 56 minutes of waiting time, the droplet form began to deteriorate and measurements could not be made. The water in the drop evaporated completely at 67 minutes. It was observed after evaporation that salt residues accumulated as a stack and ring on the solid surface. When the residual forms of the droplets after evaporation were examined, it was seen that none of them was alike. The contact angle, baseline and height change functions are obtained according to the waiting time. In particular, it was observed that the baseline and height changes showed a nearly linear change. The performed contact angle measurement system has the flexibility to be easily used in many multidisciplinary studies. It is thought that the newly developed full angle method (FAM) will create a different perspective on scientific studies.


1. Z. Xu, An exact model based dynamic contact angle algorithm. *Measurement* . **129** (2018) 611-624. https://doi.org/10.1016/j.measurement.2018.07.082.
2. A. Márquez-Herrera, M. Zapata-Torres, and S. Montesinos, Evaluation of an electrochemical cell 3D-printed with PLA/PTFE polymer filament. *Revista Mexicana de Fisica* . **68** (2022) 041002. https://doi.org/10.31349/RevMexFis.68.041002.
3. M. Danish *et al.*, Surface measurement of binderless biocomposite particleboard through contact angle and fractal surfaces. *Measurement*. **140** (2019) 365-372. https://doi.org/10.1016/j.measurement.2019.03.049.
4. J. Ma *et al.*, Superhydrophobic metallic glass surface with superior mechanical stability and corrosion resistance. *Applied Physics Letters* . **104** (2014) 173701. https://doi.org/10.1063/1.4874275.
5. Q. Wang, J. Wu, G. Meng, Y. Wang, Z. Liu, and X. Guo, Preparation of novel cotton fabric composites with pH controlled switchable wettability for efficient water-in-oil and oil-in-water emulsions separation. *Applied Physics A* . **126** (2018) 1-12. https://doi.org/10.1007/s00339-018-1781-4.
6. R. Castrejón-García, J. R. Castrejón-Pita, G. D. Martin, and I. M. Hutchings, The shadowgraph imaging technique and its modern application to fluid jets and drops. *Rev. Mex. Fis.* **57** (2011) 266-275.
7. S. Kim, T. Wang, L. Zhang, and Y. Jiang, Droplet impacting dynamics on wettable, rough and slippery oil-infuse surfaces. *Journal of Mechanical Science and Technology*. **34** (2020) 219-228. https://doi.org/10.1007/s12206-019-1223-z.
8. K. Kotra-Konicka, J. Kalbarczyk, and J. M. Gac, Modification of polypropylene membranes by ion implantation. *Chemical and Process Engineering* . **37** (2016) 331, https://doi.org/10.1515/cpe-2016-0027.
9. D. Zheng, M. Wang, M. Wang, M. Zhai, and W. Wang, Measurement of droplet size and velocity based on a single tapered fiber optical reflectometer. *Measurement* . **189** (2022) 110487, https://doi.org/10.1016/j.measurement.2021.110487.
10. C. O'Connell, *et al*., Investigation of the hydrophobic recovery of various polymeric biomaterials after 172 nm UV treatment using contact angle, surface free energy and XPS measurements. *Applied Surface Science* . **255** (2009) 4405, https://doi.org/10.1016/j.apsusc.2008.11.034.
11. G. Hodgson, M. Passmore, M. Skarysz, A. Garmory, and F. Paolillo, Contact angle measurements for automotive exterior water management. *Experiments in Fluids* . **62** (2021) 1, https://doi.org/10.1007/s00348-021-03219-2.
12. F. Rupp, L. Liang, J. Geis-Gerstorfer, L. Scheideler, and F. Hüttig, Surface characteristics of dental implants: A review. *Dental materials*. **34** (2018) 40, https://doi.org/10.1016/j.dental.2017.09.007.
13. X. Q. Du, Y. W. Liu, and Y. Chen, Enhancing the corrosion resistance of aluminum by superhydrophobic silane/graphene oxide coating. *Applied Physics A* . **127** (2021) 1-11. https://doi.org/10.1007/s00339-021-04730-3.
14. L. Mazzola, and G. Bruno, Characterization of ice-phobic surfaces: Improvements on contact angle measurements. *Measurement* . **110** (2017) 202-210. https://doi.org/10.1016/j.measurement.2017.06.036.
15. A. Marmur, C. Della Volpe, S. Siboni, A. Amirfazli, and J. W. Drelich, Contact angles and wettability: towards common and accurate terminology. *Surface Innovations* . **5** (2017) 3-8. https://doi.org/10.1680/jsuin.17.00002.
16. A. Jagadisan, and Z. Heidari, Molecular dynamic simulation of the impact of thermal maturity and reservoir temperature on the contact angle and wettability of kerogen. *Fuel* . **309** (2022) 122039. https://doi.org/10.1016/j.fuel.2021.122039.
17. J. W. Drelich *et al*., Contact angles: History of over 200 years of open questions. *Surface Innovations* . **8** (2019) 3-27, https://doi.org/10.1680/jsuin.19.00007.
18. M. Bakala, R. Wojciechowski, D. Sankowski, and A. Rylski, Semi-automatic apparatus for measuring wetting properties at high temperatures. *Metrology and Measurement Systems*. **24** (2017). https://doi.org/10.1515/mms-2017-004.
19. Y. L. Hung, Y. Y. Chang, M. J. Wang, and S. Y. Lin, A simple method for measuring the superhydrophobic contact angle with high accuracy. *Review of Scientific Instruments* . **81** (2010) 065105. https://doi.org/10.1063/1.3449325.

20. G. Whyman, E. Bormashenko, and T. Stein, The rigorous derivation of Young, Cassie-Baxter and Wenzel equations and the analysis of the contact angle hysteresis phenomenon. *Chemical Physics Letters*. **450** (2008) 355-359. https://doi.org/10.1016/j.cplett.2007.11.033.

21. M. Karhan, M. F. Çakır, and Ö. Arslan, Investigation of the effect of roughness value on the wettability behavior under electric field in XLPE materials used in medium and high voltage applications. *Electrical Engineering* . **103** (2021) 3225-3238. https://doi.org/10.1007/s00202-021-01326-1.

22. A. Sudeepthi, L. Yeo, and A. K. Sen, Cassie-Wenzel wetting transition on nanostructured superhydrophobic surfaces induced by surface acoustic waves. *Applied Physics Letters* . **116** (2020) 093704. https://doi.org/10.1063/1.5145282.

23. M. F. Çakır, An inexpensive contact angle measurement system. *Rev. Mex. Fis*. **68** (2022) 1, https://doi.org/10.31349/RevMexFis.68.021001.